New Series of Multifunctionalized Nickel(II)-Cyclam (Cyclam = 1,4,8,11-Tetraazacyclotetradecane) Complexes. Application to the Photoreduction of Carbon Dioxide

Eiichi Kimura,* Senji Wada, Mitsuhiko Shionoya, and Yohko Okazaki

Department of Medicinal Chemistry, School of Medicine, Hiroshima University, Kasumi 1-2-3, Minami-ku, Hiroshima 734, Japan

*Received June 29, 1993**

Two types of Ni^{II}–cyclam complex (cyclam = 1,4,8,11-tetraazacyclotetradecane) have been synthesized for CO_2 photoreduction catalysis. The first type (**4a**, [Ni^{II}(6-((*N*-methylpyridin-4-yl)methyl)-1,4,8,11-tetraazacyclotetradecane)]; **4b**, [Ni^{II}(6-((*N*-(*p*-methoxybenzyl)pyridin-4-yl)methyl)-1,4,8,11-tetraazacyclotetradecane)]; **4c**, [Ni^{II}-(6-((*N*-benzylpyridin-4-yl)methyl)-1,4,8,11-tetraazacyclotetradecane)]; **4d**, [Ni^{II}(6-((*N*-(*p*-nitrobenzyl)pyridin-4-yl)methyl)-1,4,8,11-tetraazacyclotetradecane)]) bear a quaternary pyridinium pendant moiety as a potential electron acceptor. The reduction potential of each cationic pyridinium moiety was found to be more positive than the respective Ni^{II} center. Their catalytic behavior toward the photoreduction of CO_2 with $Ru(bpy)_3^{2+}$ as a photosensitizer was examined in ascorbate buffer (pH 5.1, 0.1 M) and the evolved amounts of CO by **4a–d** were respectively, 3, 5.3, 5.8, and 5.1 times greater than that from underivatized Ni^{II}–cyclam (**1**). A close correlation was found between the reduction potential of each pyridinium cation and the quantity of CO evolved. As a second type of Ni^{II} complex, a new bifunctional supermolecule $Ru(bpy)_2$(bpy-py-cyclam-Ni^{II}) (**5**) (bpy-py-cyclam = (6-((*N*-((4′-methyl-2,2′-bipyridin-4-yl)methyl)pyridin-4-yl)methyl)-1,4,8,11-tetraazacyclotetradecane) has been synthesized, and its spectroscopic, redox, and CO_2 catalytic properties have been investigated. The lifetime of the excited state of **5** is long enough to permit reductive quenching in the presence of ascorbate. Although this process induced reductive photocleavage of **5**, catalytic studies show that twice the amount of CO is produced compared with a multimolecular system composite of $Ru(bpy)_3^{2+}$, pyridinium salt, and Ni^{II}–cyclam (**1**).

Introduction

There is a great deal of current interest in the fixation and activation of CO_2 by transition-metal complexes[1-9] because of the relevance to natural photosynthesis. Fisher and Eisenberg[6] were the first to show that various Co^{III} and Ni^{II} tetraazamacrocycle complexes exhibited catalytic activity for the reduction of CO_2 to CO in CH_3CN/H_2O (v/v = 1/2) or H_2O alone. Beley *et al.*[7] have since reported the remarkable ability of Ni^{II}–cyclam (**1**) to electrochemically reduce CO_2 (cyclam = 1,4,8,11-tetraazacyclotetradecane), and generate CO with high selectivity. A homogeneous aqueous system for the photoreduction of CO_2 has been reported by Grant *et al.*,[8] which utilizes Ni^{II}–cyclam (**1**) as the reduction catalyst, $Ru(bpy)_3^{2+}$ (bpy = 2,2′-bipyridine) as a photosensitizer, and ascorbate as a sacrificial electron donor. One drawback in homogeneous multimolecular systems of this type is that they lack high selectivity for production of CO over H_2 and exhibit a low quantum yield of the product CO because of other unidentified competing processes in the catalytic cycle.

In earlier studies directed toward the development of transition-metal–macrocyclic complexes as CO_2 reduction catalysts, we devised the two Ru^{II}–Ni^{II} heteronuclear complexes **2** and **3**, in

* Abstract published in *Advance ACS Abstracts,* January 15, 1994.

(1) (a) Taniguchi, I. In *Modern Aspects of Electrochemistry*; Bockris, J. O., White, R. E., Conway, B. E., Eds.; Plenum Publishing Co.: New York, 1989. (b) Collin, J.-P.; Sauvage, J.-P. *Coord. Chem. Rev.* **1989**, *93*, 245. (c) Culter, A. R.; Hanna, P. K.; Vites, J. C. *Chem. Rev.* **1988**, *88*, 1363. (d) Braunstein, P.; Matt, D.; Nobel, D. *Chem. Rev.* **1988**, *88*, 747. (e) Behr, A. *Angew. Chem., Int. Ed. Engl.* **1988**, *27*, 661. (f) Walther, D. *Coord. Chem. Rev.* **1987**, *79*, 135. (g) *Organic and Bioorganic Chemistry of Carbon Dioxide*; Inoue, S., Yamazaki, N., Eds.; Kodansha: Tokyo, 1981.

(2) (a) Matsuoka, S.; Yamamoto, K.; Ogata, T.; Kusaba, M.; Nakashima, N.; Fujita, E.; Yanagida, S. *J. Am. Chem. Soc.* **1993**, *115*, 601. (b) Matsuoka, S.; Yamamoto, K.; Pac, C.; Yanagida, S. *Chem. Lett.* **1991**, 2099. (c) Ishida, H.; Terada, T.; Tanaka, K.; Tanaka, T. *Inorg. Chem.* **1990**, *29*, 905. (d) Silavwe, N. D.; Goldman, A. S.; Ritter, R.; Tyler, D. R. *Inorg. Chem.* **1989**, *28*, 1231. (e) Ishida, H.; Tanaka, K.; Tanaka, T. *Chem. Lett.* **1988**, 339. (f) Ishida, H.; Tanaka, K.; Tanaka, T. *Chem. Lett.* **1987**, 1035. (g) Hukkanen, H.; Pakkanen, T. T. *Inorg. Chim. Acta* **1986**, *114*, L43. (h) Hawecker, J.; Lehn, J.-M.; Ziessel, R. *Helv. Chim. Acta* **1986**, *69*, 1990. (i) Ziessel, R.; Hawecker, J.; Lehn, J.-M. *Helv. Chim. Acta* **1986**, *69*, 1065. (j) Keene, F. R.; Creutz, C.; Sutin, N. *Coord. Chem. Rev.* **1985**, *64*, 247. (k) Sullivan, B. P.; Meyer, T. J. *J. Chem. Soc., Chem. Commun.* **1984**, 1244. (l) Hawecker, J.; Lehn, J.-M.; Ziessel, R. *J. Chem. Soc., Chem. Commuh.* **1984**, 328. (m) Hawecker, J.; Lehn, J.-M.; Ziessel, R. *J. Chem. Soc., Chem. Commun.* **1983**, 536. (n) Kitamura, N.; Tazuke, S. *Chem. Lett.* **1983**, 1109.

(3) (a) Morgenstern, D. A.; Wittrig, R. E.; Fanwick, P. E.; Kubiak, C. P. *J. Am. Chem. Soc.* **1993**, *115*, 6470. (b) Komeda, N.; Nagao, H.; Matsui, T.; Adachi, G.; Tanaka, K. *J. Am. Chem. Soc.* **1992**, *114*, 3625. (c) Amatore, C.; Jurand, A. *J. Am. Chem. Soc.* **1991**, *113*, 2819. (d) Dérien, S.; Duñach, E.; Périchon, J. *J. Am. Chem. Soc.* **1991**, *113*, 8447. (e) Hammouche, M.; Lexa, D.; Momenteau, M.; Savéant, J.-M. *J. Am. Chem. Soc.* **1991**, *113*, 8455. (f) Ratliff, K. S.; DeLaet, D. L.; Gao, J.; Fanwick, P. E.; Kubiak, C. P. *Inorg. Chem.* **1990**, *29*, 4022. (g) Rasmussen, S. C.; Richter, M. M.; Yi, E.; Place, H.; Brewer, K. J. *Inorg. Chem.* **1990**, *29*, 3926. (h) Ishida, H.; Fujiki, K.; Ohba, K.; Tanaka, K.; Terada, T.; Tanaka, T. *J. Chem. Soc., Dalton Trans.* **1990**, 2155. (i) DeLaet, D. L.; Lemke, F. R.; Gao, J.; Kubiak, C. P. *J. Am. Chem. Soc.* **1988**, *110*, 6904. (j) DuBois, D. L.; Miedaner, A. *J. Am. Chem. Soc.* **1987**, *109*, 113. (k) Sullivan, B. P.; Bolinger, C. M.; Conrad, D.; Vining, W. J.; Meyer, T. J. *J. Chem. Soc., Chem. Commun.* **1985**, 1414. (l) O'Toole, T. R.; Margerum, L. D.; Westermoreland, T. D.; Vining, W. J.; Murray, R. W.; Meyer, T. J. *J. Chem. Soc., Chem. Commun.* **1984**, 1244.

(4) (a) Creutz, C.; Schwarz, H. A.; Wishart, J. F.; Fujita, E.; Sutin, N. *J. Am. Chem. Soc.* **1991**, *113*, 3361. (b) Fujita, E.; Creutz, C.; Sutin, N.; Szalda, D. J. *J. Am. Chem. Soc.* **1991**, *113*, 343. (c) Schmidt, M. H.; Miskelly, G. M.; Lewis, N. S. *J. Am. Chem. Soc.* **1990**, *112*, 3420. (d) Gangi, D. A.; Durand, R. R. *J. Chem. Soc., Chem. Commun.* **1986**, 697.

(5) Sakaki, S. *J. Am. Chem. Soc.* **1992**, *114*, 2055.

(6) Fisher, B.; Eisenberg, R. *J. Am. Chem. Soc.* **1980**, *102*, 7361.

(7) (a) Beley, M.; Collin, J.-P.; Ruppert, R.; Sauvage, J.-P. *J. Chem. Soc., Chem. Commun.* **1984**, 1315. (b) Beley, M.; Collin, J.-P.; Ruppert, R.; Sauvage, J.-P. *J. Am. Chem. Soc.* **1986**, *108*, 7461.

(8) (a) Grant, J. L.; Goswami, K.; Spreer, L. O.; Otvos, J. W.; Calvin, M. *J. Chem. Soc., Dalton Trans.* **1987**, 2105. (b) Craig, C. A.; Spreer, L. O.; Otvos, J. W.; Calvin, M. *J. Phys. Chem.* **1990**, *94*, 7957.

(9) (a) Kimura, E.; Bu, X.; Shionoya, M.; Wada, S.; Maruyama, S. *Inorg. Chem.* **1992**, *31*, 4542. (b) Kimura, E.; Wada, S.; Shionoya, M.; Takahashi, T.; Iitaka, Y. *J. Chem. Soc., Chem. Commun.* **1990**, 397. (c) Shionoya, M.; Kimura, E.; Iitaka, Y. *J. Am. Chem. Soc.* **1990**, *112*, 9237.

0020-1669/94/1333-0770$04.50/0

which the photosensitizer, $Ru(bpy)_3^{2+}$ or $Ru(phen)_3^{2+}$ (phen = 1,10-phenanthroline) is covalently attached to a Ni^{II}–cyclam complex.[9] The idea was to improve the efficiency of electron transfer from the photoexcited photosensitizer to the catalytic site by covalently linking the two functional complexes. However, **2** did not work as well as expected,[9b] due to the unusual trans I configuration of the Ni^{II}–cyclam subunit and the resulting steric hindrance which impeded CO_2 access to the Ni^{II}–cyclam catalytic site and to the distortion of the coordination environment of the $Ru(bpy)_3^{2+}$ subunit and the resulting short lifetime of the excited state of the $Ru(bpy)_3^{2+}$ moiety.[10] In complex **3**, the Ni^{II}–cyclam subunit has the normal trans III configuration and there is no distortion around the Ru^{II} center of the $Ru(phen)_3^{2+}$ subunit because Ni^{II}–cyclam is attached to the phenanthroline ring via the C-5 position. However, the emission lifetime of the $Ru(phen)_3^{2+}$ is not long enough to permit the effective reductive quenching of the excited state of the $Ru(phen)_3^{2+}$ subunit by a reductant.[9a]

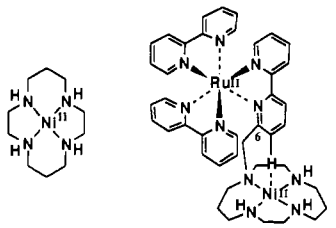

1 2

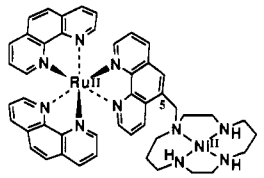

3

We report here the syntheses of novel Ni^{II}–cyclam complexes (**4a–d** and **5**) containing a pendant pyridinium group, which had been shown to function as an effective electron mediator in the photochemical reduction of H_2O by a Pt colloid.[11] The catalytic properties of these complexes for CO_2 photoreduction have been investigated, and it has been found that they provide improved efficiencies in the reduction of CO_2 and that the volume of CO evolved increases as the reduction potential of the pendant pyridinium becomes more positive.

Experimental Section

Materials. All the starting materials for synthesis were obtained commercially and were used without further purification. Analytical-grade acetonitrile was used for electrochemical and spectroscopic measurements. Tetra-*n*-butylammonium perchlorate (*n*-Bu_4NClO_4) used in electrochemical measurement was of analytical grade. The preparation of 4-(bromomethyl)-4′-methyl-2,2′-bipyridine followed the procedure of Gould *et al.*[12] $[Ni^{II}(cyclam)](ClO_4)_2$ was prepared by recrystallization of $Ni^{II}(cyclam)Cl_2$[13] from water in the presence of excess $NaClO_4$. $[Ru(bpy)_3](ClO_4)_2$ was prepared by recrystallization of $[Ru(bpy)_3]Cl_2{\cdot}6H_2O$[14] from water in the presence of excess $NaClO_4$. Metal complexes were characterized by UV–vis, IR, and ^{1}H-NMR spectroscopy and elemental analysis. Thin-layer chromatography (TLC) was carried out on Merck Art. 5554 (silica gel) TLC plates. Column chromatography was carried out using silica gel (Wakogel C-300).

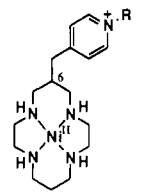

R

4a	Methyl
4b	*p*-Methoxybenzyl
4c	Benzyl
4d	*p*-Nitrobenzyl

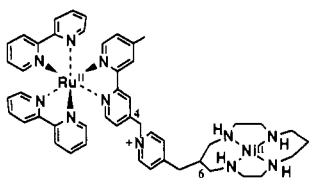

5

Caution! All the perchlorate salts used in this study may be explosive and are potentially hazardous.

Instrumentation. ^{1}H-NMR spectra were obtained on a JEOL GX-400 spectrometer (400MHz, 25 °C). 3-(Trimethylsilyl)propionic-*2,2,3,3-d*$_4$ acid, sodium salt (Merck), in D_2O and tetramethylsilane (Merck) in $CDCl_3$ were used as internal references. IR spectra were obtained on a Shimadzu FTIR-4200 spectrometer. Absorption spectra at 25.0 ± 0.1 °C were measured on a Hitachi U-3200 doublebeam spectrometer in acetonitrile or H_2O for dilute (10^{-4}–10^{-5} M) solutions of the samples, using matched quartz cells of 2-, 10-mm path length. Melting points were determined using a Yanako micro melting point apparatus and were uncorrected. Elemental analyses of C, H, and N were performed on a Yanaco CHNcorder MT-3.

Preparation of Diethyl (Pyridin-4-ylmethyl)malonate (6). A mixture of 4-picolyl chloride obtained by neutralization of the hydrochloride salt (19.7 g, 0.12 mol) with 10% $NaHCO_3$ aqueous solution, diethyl malonate (55.7 g, 0.35 mol), and anhydrous K_2CO_3 (30 g, 0.22 mol) in *N,N*-dimethylformamide (300 mL) was stirred at room temperature for 2 days. The reaction mixture was poured into ice–water (1.2 L) and extracted with several portions of ethyl acetate. The combined organic layer was extracted with 5% aqueous HCl solution (200 and 50 mL) and then the aqueous layer was neutralized with $NaHCO_3$ and extracted with dichloromethane (100 mL × 4). The combined extract was dried over $MgSO_4$ and the solvent was removed under reduced pressure. The residual oil was purified by silica gel column chromatography (eluent, AcOEt/*n*-hexane = 1/3) to obtain 21 g of diethyl (pyridin-4-ylmethyl)malonate (**6**) as a pale yellow oil (yield 70%). ^{1}H-NMR ($CDCl_3$): δ 1.22 (6H, t, J = 7.06 Hz), 3.21 (2H, d, J = 7.69 Hz), 3.66 (1H, t, J = 7.79 Hz), 4.12∼4.22 (4H, m), 7.15 (2H, dd, J = 4.4, 1.65 Hz), 8.51 (2H, dd, J = 4.4, 1.65 Hz).

Preparation of 6-(Pyridin-4-ylmethyl)-5,7-dioxo-1,4,8,11-tetraazacyclotetradecane (7a). Refluxing **6** (19.7 g, 78 mmol) and 1,9-diamino-3,7-diazanonane (2,3,2-tet) (12.6 g, 79 mmol) in 1.6 L of MeOH for 3 days afforded 6-(pyridin-4-ylmethyl)-5,7-dioxo-1,4,8,11-tetraazacyclotetradecane (**7a**) as colorless needles (14.1 g, 57% yield), followed by purification by silica gel column chromatography (eluent, CH_2Cl_2–CH_3OH–28% aqueous NH_3, 25:10:1) and recrystallization from 2-PrOH. Mp: 235–236 °C. ^{1}H-NMR ($CDCl_3$): δ 1.65 (2H, m) 2.56–2.82 (6H, m) 3.18–3.28 (4H, m) 3.48–3.58 (2H, m) 6.67 (2H, br) 7.15 (2H, dd, J = 1.64, 4.6 Hz) 8.49 (2H, dd, J = 1.65, 4.4 Hz).

Preparation of 6-(Pyridin-4-ylmethyl)-1,4,8,11-tetraazacyclotetradecane (7b). Reduction of **7a** (1.0 g, 3.1 mmol) with diborane (B_2H_6) in tetrahydrofuran (THF) (1.0 M, Aldrich) and subsequent treatment with aqueous HCl yielded 6-(pyridin-4-ylmethyl)-1,4,8,11-tetraazacyclotetradecane (**7b**) (1.20 g) as its pentahydrochloride salt in 79% yield after recrystallization from aqueous HCl–EtOH. Anal. Calcd (found) for $C_{16}H_{29}N_5{\cdot}5HCl{\cdot}H_2O$: C, 39.08 (39.38); H, 7.38 (7.18); N, 14.24 (14.31). Dec pt: 228–230 °C. IR (KBr pellet): 3470, 2877, 1640, 1601, 1509, 1456, 1373, 1219, 1070, 1035, 783, 750 cm^{-1}. ^{1}H-NMR (D_2O): δ 1.88 (2H, m) 2.39 (1H, m) 2.78 (2H, d, J = 7.33 Hz) 3.0 (16H, br) 7.47 (2H, d, J = 6.05 Hz) 8.51 (2H, d, J = 5.86 Hz).

(10) Fujita, E.; Milder, S. J.; Brunschwig, B. S. *Inorg. Chem.* **1992**, *31*, 2079.
(11) Harriman, A.; Millward, G.-R.; Neta, P.; Richoux, M. C.; Thomas, J. M. *J. Phys. Chem.* **1988**, *92*, 1286.
(12) Gould, S.; Strouse, G. F.; Meyer, T. J.; Sullivan, B. P. *Inorg. Chem.* **1991**, *30*, 2942.
(13) Bosnich, B.; Tobe, M. L.; Webb, G. A. *Inorg. Chem.* **1965**, *4*, 1109.
(14) Palmer, R. A.; Piper, T. S. *Inorg. Chem.* **1966**, *5*, 864.

Preparation of [Ni^{II}(6-(pyridin-4-ylmethyl)-1,4,8,11-tetraazacyclotetradecane)]$(ClO_4)_2$ (8). **7b**·5HCl (143 mg, 0.3 mmol) and $NiCl_2·6H_2O$ (71.8 mg, 0.3 mmol) were dissolved in 10 mL of H_2O at 80 °C, and the mixture was adjusted to pH 7 with 0.1 M NaOH aqueous solution. An excess amount of $NaClO_4$ was added to the solution, which was then allowed to stand for several days at room temperature to obtain 116 mg of orange needles as the perchlorate salt of **8** in 68% yield. Anal. Calcd (found) for **8**·$(ClO_4)_2·H_2O$, $C_{16}H_{29}N_5O_8Cl_2Ni_1·H_2O$: C, 33.89 (34.02); H, 5.51 (5.48); N, 12.35 (12.42). IR (KBr pellet): 3418, 3206, 2905, 2867, 2855, 1605, 1458, 1412, 1001, 943, 880, 797 cm^{-1}.

Preparation of [Ni^{II}(6-((*N*-methylpyridin-4-yl)methyl)-1,4,8,11-tetraazacyclotetradecane)]$(PF_6)_3$ (4a). A mixture of Ni^{II} complex **8** (99 mg, 0.18 mmol) and methyl iodide (50 mg, 0.35 mmol) in 7.5 mL of acetonitrile was stirred at room temperature for 1 day. The solvent was partially removed under reduced pressure. An aqueous solution of NH_4PF_6 was then added to the mixture to obtain light green needles of [**4a**$(CH_3CN)_2$]$(PF_6)_3$. The crystalline solid was slowly recrystallized from water containing an excess amount of NH_4PF_6 to obtain orange needles of **4a**$(PF_6)_3·H_2O$ (104 mg, 72% yield). Anal. Calcd (found) for **4a**$(PF_6)_3·H_2O$, $C_{17}H_{32}N_5P_3F_{18}Ni_1·H_2O$: C, 24.96 (25.25); H, 4.19 (4.42); N, 8.56 (8.64). IR (KBr pellet): 3440, 3218, 2955, 2880, 1653, 1474, 1300, 1194, 1176, 1098, 1063, 1049, 1018, 965 cm^{-1}.

Preparation of Ni^{II} Complexes (4b–d). All complexes were similarly prepared as follows. In a typical run, a mixture of **8** (110 mg, 0.2 mmol) and excess benzyl bromide (230 mg, 1.3 mmol) in 9 mL of acetonitrile was stirred at room temperature for 1 day. The mixture was reduced in volume under reduced pressure and then poured into water (50 mL). The water layer was washed with 50 mL of dichloromethane and 50 mL of ethyl acetate and then evaporated under reduced pressure. $NaClO_4$ aqueous solution was added to the residual mixture to obtain pale yellow needles of **4c**$(ClO_4)_3$ (122 mg, 80% yield). Anal. Calcd (found) for **4c**$(ClO_4)_3$, $C_{23}H_{36}N_5O_{12}Cl_3Ni_1$: C, 37.35 (37.12); H, 4.91 (4.88); N, 9.47 (9.47). IR (KBr pellet): 3405, 3212, 2944, 2888, 1642, 1474, 1456, 1020, 895 cm^{-1}. **4b** was prepared from **8** and *p*-methoxybenzyl chloride at reflux for 7 h as **4b**$(ClO_4)_3·H_2O$ in 62% yield. Anal. Calcd (found) for **4b**$(ClO_4)_3·H_2O$, $C_{24}H_{40}N_5O_{14}Cl_3Ni_1$: C, 36.60 (36.73); H, 5.12 (5.00); N, 8.89 (8.99). IR (KBr pellet): 3462, 3211, 2930, 1642, 1612, 1512, 1469, 1308, 1258, 895, 883, 824, 772 cm^{-1}. **4d** was prepared from **8** and *p*-nitrobenzyl bromide as **4d**$(ClO_4)_3$ in 63% yield. Anal. Calcd (found) for **4d**$(ClO_4)_3$, $C_{23}H_{35}N_5O_{14}Cl_3Ni_1$: C, 35.21 (35.12); H, 4.50 (4.42); N, 10.71 (10.74). IR (KBr pellet): 3424, 3204, 3127, 3059, 2870, 1642, 1608, 1524, 1296, 883, 806, 735, 693 cm^{-1}.

Preparation of [Bpy-py-cyclamNi^{II}]$(PF_6)_3$ (9) (bpy-py-cyclam = (6-((*N*-(4′-methyl-2,2′-bipyridin-4-yl)methyl)pyridin-4-yl)methyl)-1,4,8,11-tetraazacyclotetradecane). A mixture of **8** (99 mg, 0.18 mmol) and an excess of 4-(bromomethyl)-4′-methyl-2,2′-bipyridine (237 mg, 0.9 mmol) in 9 mL of acetonitrile was stirred at room temperature for 1 day. The reaction mixture was reduced in volume under reduced pressure and then was poured into 60 mL of water, washed with 60 mL of dichloromethane and 60 mL of ethyl acetate, and then evaporated in vacuo. The residue was poured into 20 mL of H_2O–CH_3CN (v/v = 10/1), to which an aqueous solution of NH_4PF_6 was slowly added to obtain pale yellow needles of **9**$(PF_6)_3$ (147 mg, 80% yield). Anal. Calcd (found) for **9**$(PF_6)_3·H_2O·CH_3CN$, $C_{28}H_{40}N_7P_3F_{18}Ni_1·H_2O·CH_3CN$: C, 35.07 (35.12); H, 4.41 (4.45); N, 10.91 (11.08). IR (KBr pellet): 3443, 2928, 1645, 1599, 1123, 1096, 667, 623 cm^{-1}.

Preparation of [Ru^{II}(bpy)$_2$(bpy-py-cyclamNi^{II})]$(PF_6)_5$ (5). A mixture of **9** (86 mg, 0.084 mmol) and $Ru(bpy)_2Cl_2$ (40.5 mg, 0.084 mmol) in 15 mL of EtOH-H_2O (v/v = 2/1) under Ar was heated at reflux for 10 h. The reaction was monitored by TLC (silica gel, eluent: 10% NaCl/CH_3OH/28% aqueous NH_3 = 10/2/1, R_f = 0.5, bright orange color). After evaporation, an aqueous solution of NH_4PF_6 was added to the aqueous reaction mixture to obtain crude **5**$(PF_6)_5$ in powder form. This was dissolved in the minimum amount of acetone, and upon addition of *n*-Bu_4NBr the bromide salt was obtained. This was collected, washed with acetone, and purified with the aid of a Sephadex CM-C25 cation exchange column with aqueous (0.0–0.6 M) NaCl as the eluent. Pure **5**$(PF_6)_5$ was obtained upon addition of NH_4PF_6 to the fraction eluted by 0.5 M NaCl (42.7 mg, yield 30%). Anal. Calcd (found) for **5**$(PF_6)_5$, $C_{48}H_{56}N_{11}P_5F_{30}Ni_1Ru_1$: C, 34.49 (34.56); H, 3.38 (3.58); N, 9.22 (9.10). IR (KBr pellet): 3441, 2948, 2874, 1644, 1622, 1604, 1466, 1447, 1242, 1170, 768 cm^{-1}. UV–vis in acetonitrile, λ_{max}: 454 nm (ϵ 1.49 × 10^4), 287 nm (ϵ 8.15 × 10^4), 244 nm (ϵ 3.00 × 10^4).

Preparation of [Ru^{II}(bpy)$_2$(4-((4-methylpyridinium-1-yl)methyl)-4′-methyl-2,2′-bipyridine)]$(ClO_4)_3$ (12). A mixture of 4-(bromomethyl)-4′-methyl-2,2′-bipyridine (52.6 mg, 0.2 mmol) and 4-methylpyridine (40 mg, 0.43 mmol) in 1 mL of acetonitrile was stirred at room temperature for 1 day. The solvent was removed under reduced pressure and the residue was then poured into water (10 mL). The aqueous solution was washed with dichloromethane (20 mL × 4) and evaporated to dryness in vacuo. After addition of 30 mL of EtOH–H_2O (v/v = 2/1) to the residue, the solution was purged with Ar for 30 min. $Ru(bpy)_2Cl_2$ (96.9 mg, 0.2 mmol) was then added to the solution, and the resulting mixture was heated at reflux for 3 h before being reduced in volume under reduced pressure. The chloride salt was purified with the aid of a Sephadex CM-C25 cation-exchange column with aqueous (0.0–0.3 M) NaCl as the eluent. Pure **12**$(ClO_4)_3·2H_2O$ was obtained upon addition of aqueous $NaClO_4$ solution to the 0.2–0.25 M fraction (115 mg, yield 56%). Anal. Calcd (found) for **12**$(ClO_4)_3·2H_2O$, $C_{38}H_{38}N_7Cl_3O_{14}Ru_1$: C, 44.56 (44.44); H, 3.76 (3.59); N, 9.57 (9.53).

Electrochemical Measurement. Cyclic voltammetry, normal pulse polarography, and differential pulse polarography were carried out using a Yanako P-1100 polarographic analyzer. A three-electrode system was employed. In acetonitrile, either a Pt rod, hanging mercury electrode, or dropping mercury electrode was used as the working electrode, along with a Pt-wire coil as the auxiliary electrode and a Ag/AgCl electrode as the reference electrode. The reference electrode was separated from the bulk of the solution by a glass frit and was immersed in an acetonitrile solution containing *n*-Bu_4NClO_4 (0.1 M). In H_2O, either a hanging mercury electrode or dropping mercury electrode was used as the working electrode, along with a Pt-wire coil as the auxiliary electrode and a saturated calomel electrode (SCE) as the reference electrode. All experiments were carried out at 25.0 ± 0.1 °C in solutions purged with pure Ar for 20 min in advance. Potentials are reported *vs* Ag/AgCl or SCE; the sweep rates were 100 and 5 mV/s for cyclic voltammetry and normal pulse polarographies, respectively. The differential pulse polarography were carried out at 5 mV/s of scan rate, pulse interval = 1 s, and 50 mV of pulse modulation. Experimental errors were within ±10 mV.

Spectroscopic Measurement. The ground-state luminescence spectra were recorded using a Shimadzu FR-5000 spectrophotometer at 25 °C and are uncorrected. Dilute (5 × 10^{-6} M) solutions of the samples in acetonitrile or H_2O were purged with Ar of high purity for 20 min and luminescence spectra were recorded under an Ar atmosphere.

The emission lifetimes were measured on a Horiba NAES-550 emission lifetime measuring instrument at room temperature using the time-correlated multiphoton counting method. Ar was bubbled through the dilute (5 × 10^{-6} M) solutions of the samples in acetonitrile or H_2O for 20 min before measuring and the solutions were kept under Ar during measurement. A pulsed Xe lamp was used as a light source. The wavelength at 450 nm for excitation was obtained by passing the Xe flash pulse through a monochrometer, and photons below 500 nm were counted using a 500 nm cutoff filter.

Continuous Photolysis. The continuous-illumination experiments were performed in a gastight photolysis cell that was custom-designed in order to allow purging and irradiation of the solution. The gastight cell was a 55-mL two-necked, flat-bottomed flask equipped with a quartz window (15 mm o.d.). The cell volume was 55 mL, of which 25 mL was occupied by gases. Samples of 30 mL (0.1 M ascorbate, pH 5.1) each contained 1 × 10^{-5} M of $Ru(bpy)_3^{2+}$, and 1.0 × 10^{-5}, 2.0 × 10^{-5}, or 4.0 × 10^{-5} M of Ni^{II} complex under a CO_2 atmosphere. Because commercially available CO_2 was contaminated with a small amount of CO, CO_2 from aqueous $NaHCO_3$ and 2 M H_2SO_4 was employed. Prior to photolysis, the sample solution was purged with CO_2 for 1 h. The internal pressure within the photolysis cell was kept at 1 atm by using syringe techniques. Continuous illuminations were performed with a 500-W xenon arc lamp (Ushio UI-501C). The light was filtered by a 350-nm cutoff filter (Toshiba UV-35) and an IR cutoff filter (0.5 M $CuSO_4$ aqueous solution, 50 mm path length). The light beam was concentrated with a converging lens and was focused on a quartz window of the cell. Gas samples (0.5 mL) were taken from the cell through a septum and a valve using a gastight syringe and analyzed by gas chromatography. Gas chromatographic analyses were performed using a Shimadzu GC-8A gas chromatography instrument (thermal conductivity detector) for H_2 analysis and a Shimadzu GC-4CMPF FID instrument (flame ionization detector) for CO analysis. A 13X-S molecular sieve column (3 m × 2.6 mm) was used with N_2 as the carrier gas for the H_2 and CO separations at 30 and 40 °C, respectively. The amounts of CO and H_2 were determined by comparison with authentic reference samples, which were commercially available.

Scheme 1

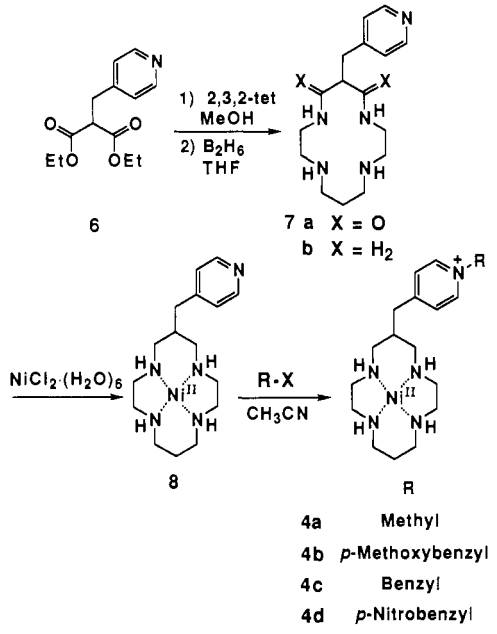

Scheme 2

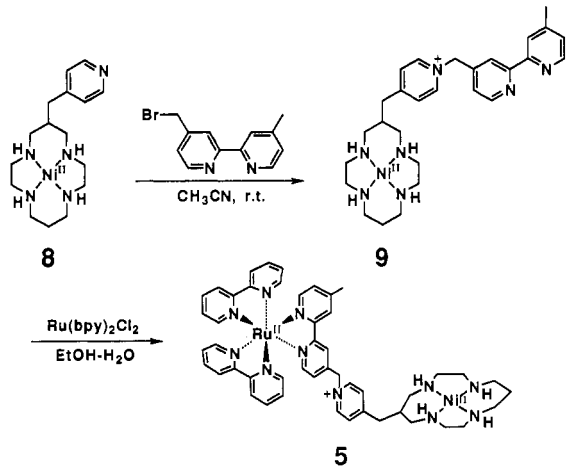

Results and Discussion

Syntheses of Pyridinium Pendant Cyclam Complexes 4a–d and 5. The new Ni^{II}–cyclams, **4a–d**, bearing a pendant pyridinium group were synthesized as shown in Scheme 1. Starting with diethyl (pyridin-4-ylmethyl)malonate (**6**) and 2,3,2-tet, we obtained the dioxocyclam **7a**. Subsequent reduction of **7a** with diborane in tetrahydrofuran yielded the new saturated macrocyclic ligand **7b**. Addition of 5 equiv of NaOH and 1 equiv of $NiCl_2·6H_2O$ to **7b**·5HCl in H_2O yielded complex **8** as an orange crystalline solid. Treatment of **8** with various alkyl halides in acetonitrile led to the Ni^{II}–cyclams with alkylpyridinium pendant, **4a–d**. All the Ni^{II} complexes, **8** and **4a–d**, were isolated as crystalline solids.

The binuclear Ru^{II}–Ni^{II} complex **5** was synthesized as summarized in Scheme 2. Treatment of **8** with 4-(bromomethyl)-4′-methyl-2,2′-bipyridine in acetonitrile at room temperature yielded the pyridinium pendant Ni^{II} complex **9** with a bpy moiety. The heterodinuclear complex **5** was prepared by refluxing **9** with $Ru(bpy)_2Cl_2$ in EtOH–H_2O (v/v = 2/1) for 10 h under Ar. Purification of **5** was performed by cation exchange column chromatography (Sephadex CM-C25) with 0.1–0.6 M NaCl aqueous solution as an eluent with the pure $5(PF_6)_5$ salt obtained upon addition of aqueous NH_4PF_6 salt to the 0.5 M NaCl fraction.

Electrochemistry of the Pyridinium Pendant Complexes. For each of the complexes **4a–d**, we expected the Ni^{II} ion center and pyridinium pendant moiety to show separate redox behavior. The electrochemical study of **4a–d** was carried out in acetonitrile solution using cyclic voltammetry, and the resulting data are listed in Table 1. The cyclic voltammograms for the oxidation of **4a–d** showed one quasi-reversible wave at +1.06 V *vs* Ag/AgCl (Figure 1a), with a peak separation of about 70–90 mV. We have assigned this redox wave to $E_{1/2}(Ni^{II/III})$ by comparison with a very similar $E_{1/2}$ value (+1.03 V *vs* Ag/AgCl) of the unsubstituted Ni^{II}–cyclam complex **1**.

The cyclic voltammograms for the reduction of **4a–c** showed one quasi-reversible wave and one irreversible cathodic peak when a hanging mercury electrode was used as the working electrode (Figure 1b), while **4a–c** showed two irreversible peaks when a Pt working electrode was used (Figure 1a). The peak potentials of the irreversible peak for **4a–c** using the hanging mercury electrode became more positive in the order **4a** < **4b** < **4c** while the quasi-reversible redox potentials of **4a–c** remained constant at −1.38 V *vs* Ag/AgCl. Both these processes have been ascribed to a one-electron reduction by comparing the height of the limiting currents for **4a–c** with **1** using polarography. The quasi-reversible waves were assigned to $E_{1/2}(Ni^{I/II})$ from a comparison with the value of $E_{1/2}(Ni^{I/II})$ for **1** (−1.39 V) and the irreversible peak to the reduction of the pyridinium cation to a pyridinium radical. (The potential of the reduction of pyridinium part for **4a** was

Table 1. Cyclic Voltammetric Data for Pyridinium-Pendant Ni^{II} Complexes in Acetonitrile and H_2O[a,b]

	in CH_3CN					
		$E_{1/2}(Ni^{I/II})$, V		$E_{1/2}(Py^{\cdot}/Py^{+})$, V		in H_2O
complex	$E_{1/2}(Ni^{II/III})$, V[a,c] (ΔE_p, mV)	Pt[e]	Hg[f]	Pt[e]	Hg[g]	E_p, V[b,d]
1	+1.03 (75)	−1.42	−1.39			−1.61 (1)
4a	+1.06 (90)	−1.49	−1.38	−1.37	−1.42[h]	−1.57 (2.09)
4b	+1.05 (75)	−1.47	−1.38	−1.33	−1.31	−1.47 (1.76)
4c	+1.06 (80)	−1.47	−1.38	−1.30	−1.29	−1.46 (1.71)
4d	+1.06 (80)	*i*	*i*	−0.91[j]	−0.86[j]	

[a] Conditions for the determination of redox potentials in acetonitrile: [Ni^{II} complex] = 5 × 10^{-4} M; [*n*-Bu_4NClO_4] = 0.1 M, sweep rate = 100 mV/s *vs* Ag/AgCl at 25 °C in acetonitrile. [b] Conditions for the determination of redox potentials in H_2O: [Ni^{II} complex] = 5 × 10^{-4} M; [Na_2SO_4] = 0.5 M; sweep rate = 5 mV/s *vs* SCE at 25 °C in H_2O. [c] $E_{1/2}(Ni^{II/III}) = (E_{cathodepeak} + E_{anodepeak})/2$ using a Pt rod electrode as the working electrode in acetonitrile. [d] Peak potential obtained by differential pulse polarography using a dropping mercury electrode as the working electrode in H_2O, modulation amplitude = 50 mV. The height of the limiting current by normal pulse polarography is given in parentheses. [e] Peak potential using a Pt rod electrode as the working electrode at a scan rate of 100 mV/s in acetonitrile. [f] $E_{1/2}(Ni^{I/II}) = (E_{cathodepeak} + E_{anodepeak})/2$ using a hanging mercury electrode as the working electrode in acetonitrile. [g] Peak potential using a hanging mercury electrode as the working electrode at a scan rate of 100 mV/s in acetonitrile. [h] The shoulder potential. [i] Not observed. [j] See text.

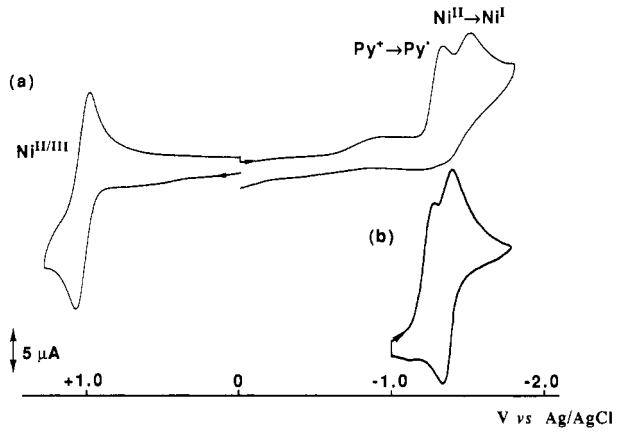

Figure 1. Cyclic voltammogram of 5 × 10^{-4} M **4c** in acetonitrile (0.1 M *n*-Bu_4NClO_4) *vs* Ag/AgCl at 25 °C, scan rate = 100 mV/s: (a) at a Pt rod electrode; (b) at a dropping mercury electrode.

obtained from the shoulder potential of the cathodic wave. Separation of the peaks corresponding to the reduction of the pyridinium cation and Ni^{II} was not observed for **4a** because the difference in reduction potentials was very small.) Lin *et al.* reported that dimerization occurs upon reduction of an *N*-methylpyridinium cation to a pyridinium radical.[15] However, it has not been confirmed whether or not this dimerization occurs for **4a–c**. The first irreversible peak values for **4a–c** using the Pt working electrode showed a similar order as before (**4a** < **4b** < **4c**) while the values for the second peak remained roughly constant. Therefore, we have assigned the first peak to the one-electron reduction of the pyridinium cation to form **10** and the second peak to the one-electron reduction of the Ni^{II} center to form **11** irreversibly. For **4d**, one irreversible peak appeared at –0.86 V *vs* Ag/AgCl using the Hg working electrode but no reduction current from Ni^{II} to Ni^{I} was observed around –1.4 V. The unexpected reduction wave with **4d** may be due to the electrochemical reduction of the *p*-nitrobenzyl group.

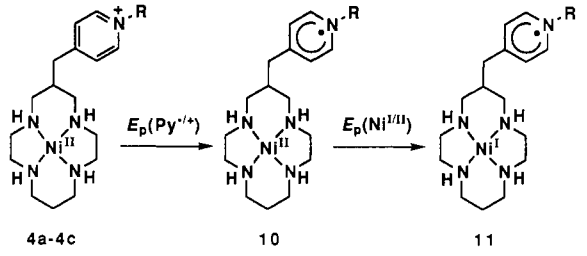

The $E_{1/2}(Ni^{I/II})$ and $E_{1/2}(Ni^{II/III})$ values for **4a–c** suggest that the Ni^{II} centers of **4a–c** retain essentially the same coordination environment as for **1**. The similar λ_{max} and molecular extinction coefficient (ϵ, M^{-1} cm^{-1}) values for the d–d absorption band of **4a–d** (**4a**, 452 nm, ϵ = 43; **4b**, 448 nm, ϵ = 41; **4c**, 452 nm, ϵ = 46; **4d**, 450 nm, ϵ = 42; **1**, 450 nm, ϵ = 46 in H_2O, I = 1.5 M, Na_2SO_4) support this notion. The reduction potential for the pyridinium cation was more positive than the reduction potential for Ni^{II} to Ni^{I}, and the peak shifted to a more positive potential in the order **4a** < **4b** < **4c**. The difference in reduction potential for the pyridinium cation in **4a–c** is due to the electron-withdrawing effect of the substituent on the pyridinium cation. These results indicate that the potential for one-electron reduction of the pyridinium ion can be controlled by changing the substituent on the pyridinium moiety.

The electrochemical behavior of **4a–c** in H_2O was also investigated using a hanging mercury electrode, and the resulting data are included in Table 1. The cyclic voltammograms of **4a–c** showed just one cathodic peak, which were found to involve two-electron reduction processes by comparing the limiting current height with that for **1** using polarography. This contrasts with the studies with **4a–c** in acetonitrile, which revealed the appearance of two distinct reduction peaks as stated earlier. The differential pulse polarograms of **4a–c** and **1** in H_2O are shown in Figure 2. The peak potentials of these differential pulse polarograms become more positive in the order of **1** < **4a** < **4b** < **4c**, and once again no peak separation between the reduction wave of the pyridinium cation and that of Ni^{II} is observed for **4a–c**. Therefore, it is likely that the cathodic peaks in the cyclic voltammograms and the differential pulse polarograms of **4a–c** are the sum of the one-electron reduction of the pyridinium cation to the pyridinium radical and the one-electron reduction of Ni^{II} to Ni^{I}. The $Ni^{I/II}$ reduction potential for **4a–c** in H_2O could be shifted to more positive values as a result of interaction between the reduced

(15) (a) Lin, C. S.; Wang, Y. Y.; Wan, C. C. *J. Chin. Inst. Eng.* **1987**, *10*, 385. (b) Yang, C. S.; Wang, Y. Y.; Wan, C. C. *J. Electrochem. Soc.* **1989**, *136*, 2592.

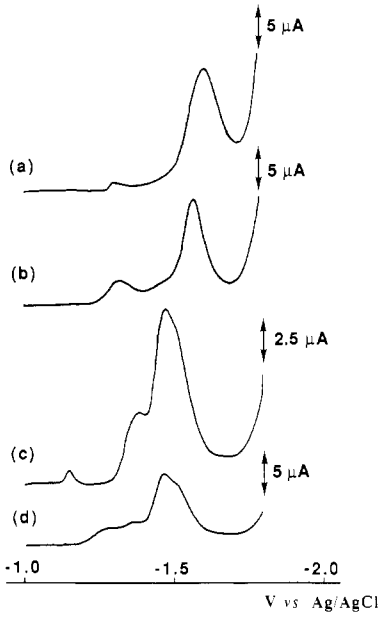

Figure 2. Differential pulse polarograms of (a) 5 × 10^{-4} M **1**, (b) 5 × 10^{-4} M **4a**, (c) 5 × 10^{-4} M **4b**, and (d) 5 × 10^{-4} M **4c** in H_2O (0.5 M Na_2SO_4) at dropping mercury electrode *vs* SCE at 25 °C.

form of the pyridinium cation and Ni^{II} (for example, the equilibrium between the pyridinium radical and Ni^{I}).[16]

Photoreduction of Carbon Dioxide by Pyridinium Pendant Complexes. Grant *et al.*[8a] reported that carbon dioxide is reduced to CO photochemically by **1** in ascorbate buffer solution in the presence of $Ru(bpy)_3^{2+}$, although the quantum yield for CO_2 reduction is low. Our experiments on the photoreduction of CO_2 with pyridinium pendant complexes (**4a–d**) were carried out with 1.0 × 10^{-5}, 2.0 × 10^{-5}, or 4.0 × 10^{-5} M concentrations of each Ni^{II} complex, $Ru(bpy)_3^{2+}$ (1.0 × 10^{-5} M) as a photosensitizer, and ascorbate buffer as a sacrificial electron donor (30 mL, 0.10 M, pH 5.1) under a CO_2 atmosphere at 25 °C. After photoirradiation with a Xe lamp (λ > 350 nm), the evolved gas was analyzed by gas chromatography for CO and H_2 and compared with authentic reference samples. Under these conditions, the plot of the amounts of CO and H_2 formed against irradiation time shows decreases in the rate of CO and H_2 production after 90 min (Figure 3). In our system, the decomposition of $Ru(bpy)_3^{2+}$ was observed during photoirradiation, which was also the case with Grant's system.[8a] The absorption intensity at 450 nm decreased by 40% after 80 min of photoirradiation.

The volumes of CO and H_2 evolved after 2 h of photoirradiation are compared among various Ni^{II} complex catalysts in Table 2. In the absence of the Ni^{II} catalyst, a trivial amount of H_2 was produced and no CO evolution was observed (run 20). However, the volumes of evolved CO increased with the concentration of

(16) To give a preliminary assessment of the catalytic abilities of **4a–d** for electrochemical reduction of CO_2, cyclic voltammogram studies at a dropping mercury electrode were carried out in the absence and in the presence of CO_2. In the presence of CO_2, Ni^{II}–cyclam showed a large catalytic wave due to the current associated with reduction of CO_2 to CO, whereas no such current was observed in the absence of CO_2. The Ni^{I}–cyclam which is adsorbed on a mercury electrode surface has previously been shown to be an active species for the electrochemical reduction of CO_2.[7b,20] Under our conditions (I = 1.5 M, Na_2SO_4, [complex] = 0.5 mM, a dropping mercury electrode as the working electrode *vs* SCE at 25 °C, scan rate = 100 mV/s), our new Ni^{II}–cyclam series showed a similar effect with large catalytic currents observed in the presence of CO_2. The peak potentials are as follows (the relative intensity *vs* the intensity of the catalytic peak of **1** is shown in parentheses): **1**, –1.38 V (1); **4a**, –1.38 V (0.98); **4b**, –1.38 V (0.94); **4c**, –1.36 V (0.61); **4d**, –1.39 V (0.97). In addition, the potentials where the catalytic current for CO_2 reduction starts for **4a–4c** are slightly more positive than that for **1**: **1**, –1.22 V; **4a**, –1.20 V; **4b**, –1.20 V; **4c**, –1.20 V; **4d**, –1.22 V. These results show that the pyridinium pendant Ni^{II}–cyclam series is effective for the electrochemical catalytic reduction of CO_2.

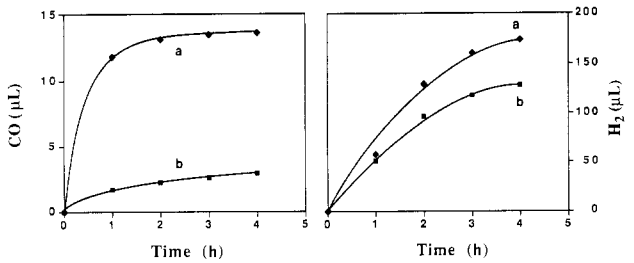

Figure 3. Generation of CO and H_2 with (a) 1×10^{-5} M **4c** and (b) 1×10^{-5} M **1** in 30 mL of 0.1 M ascorbate buffer (pH 5.1) with 1×10^{-5} M $Ru(bpy)_3^{2+}$ under a CO_2 atmosphere. The reaction mixtures were irradiated with a 500-W Xe lamp at 25 °C.

Table 2. Generation of CO and H_2 by the Photoreduction of CO_2[a]

run	complex	concn, $\times 10^{-5}$ M	amt of CO, μL	amt of H_2, μL	CO/H_2
1	**1**	1.0	2.3	111	0.020
2	**1**	2.0	4.1	122	0.034
3	**1**	4.0	5.2	75	0.070
4	**4a**	1.0	7.1	115	0.061
5	**4a**	2.0	9.4	89	0.11
6	**4a**	4.0	11.0	38	0.29
7	**4b**	1.0	12.1	118	0.10
8	**4b**	2.0	17.4	103	0.17
9	**4b**	4.0	21.5	33	0.65
10	**4c**	1.0	13.4	139	0.096
11	**4c**	2.0	18.9	93	0.20
12	**4c**	4.0	23.6	45	0.65
13	**4d**	1.0	11.8	109	0.11
14	**4d**	2.0	16.2	80	0.20
15	**4d**	4.0	17.1	15	1.13
16[b]	**1**	1.0	1.8	95	0.018
17[c]	**1**	2.0	2.1	107	0.019
18[d]	**1**	4.0	1.7	58	0.029
19[e]	**5**	1.0	4.0	32	0.13
20	none	0	0	22	0

[a] All experiments contain 1×10^{-5} M $Ru(bpy)_3^{2+}$, dissolved in 30 mL of CO_2 saturated ascorbate buffer solution (0.1 M, pH = 5.1). Irradiation was carried out for 2 h at 25 °C. [b] 1×10^{-5} M *N*-methylpyridinium hexafluorophosphate was included in the same solution as run 1. [c] Contained 2×10^{-5} M *N*-methylpyridinium hexafluorophosphate. [d] Contained 4×10^{-5} M *N*-methylpyridinium hexafluorophosphate. [e] 1×10^{-5} M **5** was contained in 30 mL of CO_2 saturated ascorbate buffer solution (0.1 M, pH = 5.1).

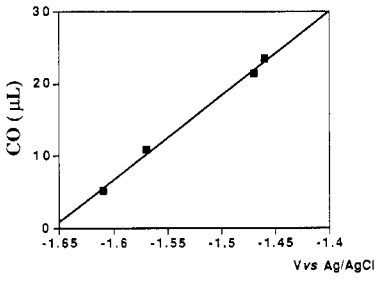

Figure 4. Relationship between the peak potentials of the differential pulse polarography for **4a–c** and **1** in H_2O and the volume of CO generated.

the Ni^{II} catalyst, whereas the volume of evolved H_2 decreased. Craig *et al.*[8b] reported that CO was predominantly produced in the photoreduction of CO_2 using high concentration of Ni^{II}–cyclam (5×10^{-3} M).

Similarities in the redox potentials of $Ni^{II/III}$ and $Ni^{I/II}$ as well as the d–d absorption properties for **1** and **4a–d** indicate that the coordination environment of the Ni^{II} center of each complex is essentially the same. However, the efficiency of these complexes in CO evolution is in the order **1** < **4a** < **4b** < **4d** < **4c**, no matter what the concentration of the Ni^{II} catalyst. Figure 4 shows the relationship between the peak potentials for the reduction of the pyridinium pendant Ni^{II}–cyclam series (determined by differential pulse polarography in H_2O) and the amounts of CO evolved after 2 h of irradiation. This result indicates that the reduction potential of the pyridinium cation is instrumental in determining the CO photoreduction yield, supporting a notion that the pyridinium cation operates as an electron acceptor. However, these pyridinium cations intermolecularly added appear to function neither as electron mediators nor as inhibitors in the reference system of $Ru(bpy)_3^{2+}$ and Ni^{II}–cyclam (runs 16 and 17).

As for the mechanism of CO and H_2 formation, the initial step would involve the absorption of light by $Ru(bpy)_3^{2+}$, followed by reductive quenching of the excited state of $Ru(bpy)_3^{2+}$ by ascorbate ion.[17]

$$Ru(bpy)_3^{2+} + h\nu \rightarrow {}^*Ru(bpy)_3^{2+} \quad (1)$$

$${}^*Ru(bpy)_3^{2+} + HA^- \rightarrow Ru(bpy)_3^{+} + HA^{\bullet} \quad (2)$$

where the HA^- is the ascorbate ion and $HA^{\bullet}$ is the protonated ascorbate radical. Formation of H_2 by irradiation of $Ru(bpy)_3^{2+}$ in ascorbate buffer solution has been previously reported.[18] There is, however, considerably more H_2 evolved in the presence of a Ni^{II} catalyst. Thus, Ni^{II}–cyclam must catalyze the reduction of H_2O to H_2. The following mechanism is proposed for the electron transfer from $Ru(bpy)_3^{+}$ in the photoreduction of CO_2:

$$Ru(bpy)_3^{+} + Py^{+}\text{–}Ni^{II}\text{cyclam} \rightarrow Ru(bpy)_3^{2+} + Py^{\bullet}\text{–}Ni^{II}\text{cyclam} \quad (3)$$

$$Ru(bpy)_3^{+} + Py^{\bullet}\text{–}Ni^{II}\text{cyclam} \rightarrow Ru(bpy)_3^{2+} + Py^{\bullet}\text{–}Ni^{I}\text{cyclam} \quad (4)$$

Here Py^+ and $Py^{\bullet}$ are the pyridinium cation and pyridinium radical parts of **4a–c**, respectively. The two-electron reduced form of the pyridinium pendant Ni^{II}–cyclam ($Py^{\bullet}$–Ni^{I}cyclam) is assumed to be an active species for the two-electron reduction of CO_2 via intramolecular electron transfer. The pyridinium pendant might work as the efficient electron acceptor and/or the efficient electron pool in the reduction process since the electrochemical studies show that the stability of the one-electron-reduced form of the pyridinium pendant Ni^{II}–cyclam ($Py^{\bullet}$–Ni^{II}cyclam) is linked to the amount of CO evolved for the pyridinium pendant Ni^{II}–cyclam series (Figure 4). In other words, the ease of pyridinium cation reduction as shown in eq 3 appears to determine the yield of evolved CO. However, the differences in H_2 evolution between these complexes are much smaller than the differences in CO evolution. Therefore further investigations are under way to determine the differences in the pathways between CO_2 and H_2O reduction.

Electrochemistry of the Ru^{II}–Ni^{II} Complex 5. The electrochemical behavior of **5** was studied in acetonitrile solution by cyclic voltammetry and differential pulse polarography using a Pt rod electrode as the working electrode, and the resulting electrochemical data are summarized in Table 3. The cyclic voltammogram for the oxidation of **5** showed two quasi-reversible waves (+1.31 and +1.06 V *vs* Ag/AgCl), which have been assigned to $E_{1/2}(Ru^{II/III})$ and $E_{1/2}(Ni^{II/III})$, respectively, from a comparison with the $E_{1/2}$ values for $Ru(bpy)_3^{2+}$ (+1.32 V) and **1** (+1.03 V). In the case of **2**, the oxidation potential from Ni^{II} to Ni^{III} was not observed.[9b] The $Ni^{II/III}$ redox potential for **3**, however, was 0.53 V more positive than that for **1**[9a] and the $Ni^{II/III}$ and $Ni^{I/II}$ potentials for the *N*-monomethylated Ni^{II}–cyclam complex[19] were shifted by +96 and +101 mV, respectively. Therefore, the reason for the lack of any shift in the $Ni^{II/III}$ redox couple for **5** must be because there are no N-substituents on the cyclam ring.

The cyclic voltammogram for the reduction of **5** showed three

(17) Creutz, C.; Sutin, N.; Brunschwig, B. S. *J. Am. Chem. Soc.* **1979**, *101*, 1297.
(18) Krishnan, C. V.; Sutin, N. *J. Am. Chem. Soc.* **1981**, *103*, 2141.
(19) Ciampolini, M.; Fabbrizzi, L.; Licchelli, M.; Perotti, A.; Pezzini, F.; Poggi, A. *Inorg. Chem.* **1986**, *25*, 4131.

Table 3. Redox Properties of Ru^{II} Complexes in Acetonitrile[a]

complex	$E_{1/2}$(Ru), V II/III[b]	I/II[c]	0/I[c]	−I/0[c]	$E_{1/2}$(Ni), V II/III[b]	I/II[d]	$E_{1/2}$ ($Py^{\bullet}/Py^{+}$)[e]
$Ru(bpy)_3^{2+}$	+1.32	−1.28	−1.48	−1.73			
5	+1.31	−1.29	−1.49	−1.76	+1.06		−1.14 (−1.07[c])
4b					+1.06	−1.38	−1.29
1					+1.03	−1.39	

[a] Conditions for the determination of redox potentials: [metal complex] = 5 × 10^{-4} M; [n-Bu_4NClO_4] = 0.1 M; sweep rate = 100 mV/s *vs* Ag/AgCl at 25 °C in acetonitrile. [b] $E_{1/2}$(II/III) = ($E_{cathodepeak}$ + $E_{anodepeak}$)/2 using a Pt rod electrode as the working electrode. [c] Peak potential determined by differential pulse polarography using a Pt rod electrode as the working electrode, modulation amplitude = 50 mV. [d] $E_{1/2}$(I/II) = ($E_{cathodepeak}$ + $E_{anodepeak}$)/2 using a hanging mercury electrode as the working electrode. [e] Peak potential using a Pt rod electrode as the working electrode at a scan rate of 100 mV/s.

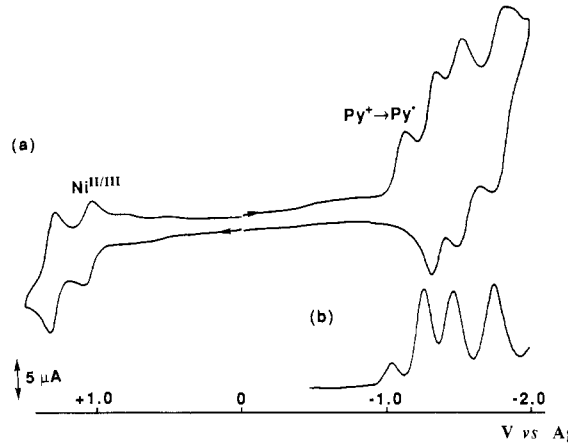

Figure 5. (a) Cyclic voltammogram of 5 × 10^{-4} M **5** at a Pt rod electrode in acetonitrile (0.1 M n-Bu_4NClO_4) *vs* Ag/AgCl at 25 °C. Scan rate = 100 mV/s. (b) Differential pulse polarograms of **5** at a Pt rod electrode in acetonitrile (0.1 M n-Bu_4NClO_4) *vs* Ag/AgCl at 25 °C.

quasi-reversible redox waves and one irreversible cathodic peak (Figure 5). This process corresponds to a four electron reduction in total from a comparison with the limiting current height for $Ru(bpy)_3^{2+}$ using polarography. The three quasi-reversible waves are attributed to $E_{1/2}(Ru^{I/II})$, $E_{1/2}(Ru^{0/I})$, and $E_{1/2}(Ru^{-I/0})$, respectively, from a comparison with the $E_{1/2}$ values for $Ru(bpy)_3^{2+}$ (−1.28, −1.48, −1.73 V *vs* Ag/AgCl). The irreversible peak is attributed to the formation of the pyridinium radical from the reduction of the pyridinium cation. This value is more positive than those found for the **4a–c** series because the pyridinium cation of **5** has a bipyridyl substituent which is considered to be an electron-deficient species.

Although the reduction of the Ni^{II} center in **5** is not apparent under these conditions, we nonetheless examined the electrochemical behavior of **5** in H_2O under a CO_2 atmosphere and compared the ability for CO_2 reduction of **5** with those of **1** and **3** under the same condition (I = 1.5 M, Na_2SO_4, [complex] = 0.5 mM, a dropping mercury electrode as the working electrode *vs* SCE at 25 °C, scan rate = 100 mV/s). The cyclic voltammogram of **3** and **5** in the absence of CO_2 showed complex behavior and did not offer meaningful information. However, the cyclic voltammograms of **1**, **3**, and **5** showed the high catalytic current due to the reduction of CO_2 to CO by the adsorbed Ni^{I} species on mercury surface[7b,20] in the presence of CO_2 by comparison with those in the absence of CO_2. The peak potentials are as followed (the relative intensity *vs* that of **1** is shown in parentheses): **1**, −1.38 V (1); **3**, −1.71 V (0.22); **5**, −1.39 V (0.53). **5** has peak potential very close to that of **1** due to the absence of the substituent on the N atom of the Ni^{II}–cyclam part, though the peak potential of **3** is negatively shifted by 330 mV. This negative shift for **3** might be due to the steric hindrance of the N-substituent on the Ni^{II}–cyclam part of **3** when the CO_2 reduction occurs.

(20) Fujihira, M.; Hirata, Y.; Suga, K. *J. Electroanal. Chem.* **1990**, *292*, 199.

Table 4. Absorption Data[a]

complex	in CH_3CN λ_{max}, nm	$10^{-4}\epsilon$, M^{-1} cm^{-1}	in H_2O λ_{max}, nm	$10^{-4}\epsilon$, M^{-1} cm^{-1}
$Ru(bpy)_3^{2+}$	451	1.4	453	1.4
	287	8.4	286	7.9
	244	2.5	244	2.5
5	454	1.5	456	1.4
	287	8.2	287	7.6
	244	3.0	245	3.5 (sh)
12	454	1.5	454	1.4
	288	8.4	287	8.0
	247	2.9	247	2.8

[a] ϵ values were determined on the basis of a single run on a Hitachi U-3200 doublebeam spectrometer using 2.5 × 10^{-5} M Ru^{II} complexes.

Table 5. Luminescence Data and Related Quantities of Ru^{II} Complexes[a]

complex	in CH_3CN emission,[b] nm (Φ_{rel})	lifetime,[c] ns	in H_2O emission,[b] nm (Φ_{rel})	lifetime,[c] ns
$Ru(bpy)_3^{2+}$	607 (1.0)	980	607 (1.0)	550
5	650 (0.46)	460	650 (0.51)	315
12	648 (1.0)	780	650 (0.66)	400

[a] All experiments were carried out using 5 × 10^{-6} M Ru^{II} complexes at room temperature under an Ar atmosphere. [b] Excitation wavelength was 450 nm. Φ_{rel} Values are relative emission intensities based on that of $Ru(bpy)_3^{2+}$ complex. [c] Excitation wavelength was 450 nm. The emission decay was followed below 500 nm.

Absorption and Emission Properties of 5. The absorption spectrum of **5** is characterized by intense bands in the UV and visible regions (Table 4). The bands centered at about 280 nm correspond to ligand-centered (^{1}LC) transitions, and the bands in the visible region (*ca.* 450 nm) correspond to metal-to-ligand charge-transfer transitions (^{1}MLCT, Ru^{II} → bpy π^*).[21] The λ_{max} and molecular extinction coefficients for the complexes $Ru(bpy)_3^{2+}$, **5**, and **12** are all very similar. Therefore, the absorption band for the Ni^{II}–cyclam moiety in **5** must have a small molar absorption coefficient (ϵ) and is concealed behind that of the very intense $Ru(bpy)_3^{2+}$ subunit (ϵ = 1.4 × 10^4).

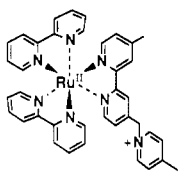

12

Compared to $Ru(bpy)_3^{2+}$, the emission maxima of **5** and **12** in H_2O are red-shifted from 607 to 650 nm (Table 5) and the emission spectra shapes of **5** and **12** are quite similar (Figure 6). These results imply that the red-shift for **5** and **12** occurs because the π^* orbital of the bpy ligand attached to the electron-withdrawing pyridinium cation[22] is of lower energy and that the Ni^{II}–cyclam part of **5** does not greatly affect the Ru^{II} coordination environment. The lifetimes of the excited state of the Ru^{II}

(21) We assigned the characteristics of the absorption spectra of the Ru^{II} complexes according to the following literature. (a) Kalyanasundaram, K. *Coord. Chem. Rev.* **1982**, *46*, 159. (b) Juris, A.; Balzani, V.; Barigelletti, F.; Campagna, S.; Belser, P.; Zelewsky, A. V. *Coord. Chem. Rev.* **1988**, *84*, 85.

(22) For the examples of the effects of the electron-withdrawing substituent for $Ru(bpy)_3^{2+}$. (a) Mabrouk, P. A.; Wrighton, M. S. *Inorg. Chem.* **1986**, *25*, 526. (b) Furue, M.; Maruyama, K.; Oguni, T.; Naiki, M.; Kamachi, M. *Inorg. Chem.* **1992**, *31*, 3792.

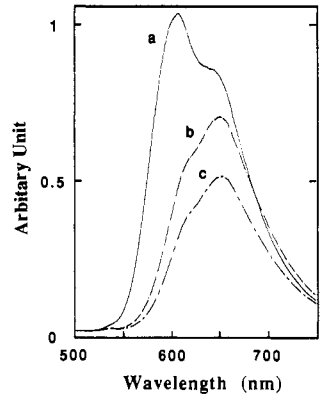

Figure 6. Emission spectra of (a) 5×10^{-6} M $Ru(bpy)_3^{2+}$, (b) 5×10^{-6} M **12**, and (c) 5×10^{-6} M **5** in H_2O at 25 °C (excitation = 450 nm).

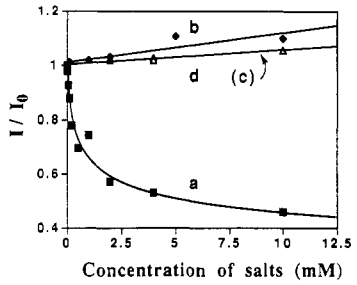

Figure 7. Salt concentration dependence of the emission intensity for **5** and **12** in H_2O at 25 °C (excitation = 450 nm). [Ru^{II} complex] = 5×10^{-6} M. I/I_0 = (the emission intensity with each concentration of salt)/(the emission intensity without salt). Key: (a, ■) **5** + NaSCN; (b, ◆) **5** + $NaClO_4$; (c, ▲) = **12** + $NaClO_4$; (d, △) **12** + NaSCN.

complexes were measured by time-correlated multiphoton counting. Although complexes **5** and **12** contain mixed chelates, each showed a single-exponential decay. The values for the lifetimes of **5** and **12** in acetonitrile agree well with the emission intensities of each Ru^{II} complex.

The relative intensity of the emission spectrum of **5** is *ca.* half that of $Ru(bpy)_3^{2+}$. In previous studies on this type of heteronuclear Ru^{II}–Ni^{II} complex, the relative intensities of the emission spectra of **2**[9a] and **3**[9b] decreased to *ca.* $^1/_{160}$ and $^1/_{20}$, respectively, of that of the parent Ru^{II} complexes, $Ru(bpy)_3^{2+}$ or $Ru(phen)_3^{2+}$. In the case of **2**, which has a very short lifetime, the emission decay processes consist of two channels:[10] a temperature-independent pathway to the ground state and a thermally-activated pathway from ^{3}MLCT to ^{3}LF of the Ru^{II} center. The activation free energy from ^{3}MLCT to ^{3}LF for the latter pathway is lower than that of the parent $Ru(bpy)_3^{2+}$ (1750–1980 cm^{-1} for **2** and 3000 cm^{-1} for $Ru(bpy)_3^{2+}$ in EtOH) due to an increase in the Ru–N bond length and the distortion of the coordination environment, and this is the main reason for the very short lifetime of the excited state of **2**. In the case of **3**, there is no coordinative distortion around the Ru^{II} center, and so the short lifetime for the excited state of **3** must be due to effective energy transfer from ^{3}MLCT to the Ni^{II} center of the Ni^{II}–cyclam subunit.[9a] The emission intensity of **5** was found to be slightly less than that of **12** and the lifetime of the excited state of **5** was also shorter than that of **12**. However, compared to **2** and **3**, the excited-state properties of **5** are not as affected by the Ni^{II}–cyclam moiety.

The changes in the emission intensities of **5** and **12** in the presence of different concentrations of $NaClO_4$ or NaSCN solution were measured (Figure 7). The emission intensity of **12** slightly increased when the concentration of $NaClO_4$ or NaSCN was raised up to 10 mM. A similar effect was observed upon the addition of $NaClO_4$ to **5**. However, the emission intensity of **5** decreased upon addition of increasing amounts of NaSCN. After addition of 2 mM of NaSCN to **5**, the relative emission intensity had decreased by 0.57-fold. Ni^{II}–cyclam is a mixture of high-spin (octahedral, 6-coordinate) and low-spin (square-planar, 4-coordinate) states in H_2O. When the SCN^- ion is present in solution, SCN^- coordination to the axial positions forms 6-coordinate Ni^{II} and so the distribution of the high-spin state increases.[23] Thus, the lower intensity of emission for **5** compared with **12** appears to be the result of effective energy transfer to the paramagnetic high-spin state of Ni^{II}–cyclam from the ^{3}MLCT excited state.

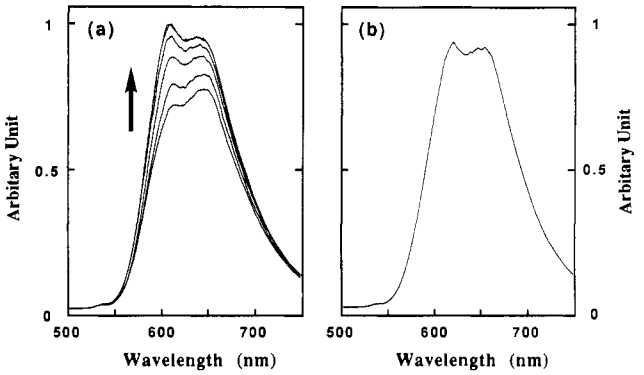

Figure 8. (a) Change of the emission spectra of **5** during photoirradiation (450 nm) with 1.0×10^{-2} M sodium ascorbate and 0.1 M $NaClO_4$ (pH = 7.0, 5.0×10^{-2} M MOPS) after 0, 10, 30, 60, 100, and 180 min. (b) Emission spectrum of 5×10^{-6} M $Ru(bpy)_2DMB$ in H_2O.

The excited-state redox potentials can be estimated by calculating on the basis of the ground-state potential and the MLCT excited energy (E_{MLCT}):[21a] $E_{1/2}(Ru^I/{}^*Ru^{II}) = E_{1/2}(Ru^{I/II}) + E_{MLCT}$ and $E_{1/2}({}^*Ru^{II}/Ru^{III}) = E_{1/2}(Ru^{II/III}) - E_{MLCT}$. Complex **5** has 1.91 eV of the MLCT excited energy calculated from the wavelength of the emission maximum (650 nm) in acetonitrile. The redox potentials for the $E_{1/2}(Ru^I/{}^*Ru^{II})$ and $E_{1/2}({}^*Ru^{II}/Ru^{IV})$ for **5** are +0.62 and –0.60 V, respectively. These values suggest that any electron transfer between $^*Ru^{II}$ and Ni^{II} (to produce the Ni^I–Ru^{III} or the Ni^{III}–Ru^I state) does not occur under photoirradiation.

Photochemical Behavior of 5 in Photoreduction of CO_2. Figure 8a shows the spectral change in the emission of **5** over 3 h of photoirradiation (wavelength = 450 nm) in 0.1 M of $NaClO_4$ solution, containing 5.0×10^{-2} M of 3-morpholinopropanesulfonic acid (MOPS) as buffer (pH = 7.0) and 1.0×10^{-2} M of sodium ascorbate as reductant under Ar. The fluorescence spectrum changed increasingly with blue-shift of the emission maximum and then within 3 h reached a constant emission. This spectral change may be due to photochemical reaction after the reductive quenching of **5** by ascorbate. The excited state of $Ru(bpy)_3^{2+}$ is reductively quenched by ascorbate ion,[17] resulting in the decrease of the emission intensity. However, the intensity does not show any further change upon longer irradiation. The photoreaction of **5** was followed by TLC, and finally the resulting crude product was obtained. After 2 h of irradiation from a Xe lamp ($\lambda > 350$ nm) to a solution of **5** (1×10^{-3} M) and sodium ascorbate (1×10^{-2} M), a new main spot on TLC (silica gel; eluent *N*,*N*-dimethylformamide/5% aqueous NH_4Cl = 10/1; R_f = 0.5 for new spot, R_f = 0.1 for **5**) had appeared and a crude precipitate was obtained upon addition of aqueous NH_4PF_6 to the solution. From a comparison with both the ^{1}H-NMR and emission spectra of $Ru(bpy)_2DMB^{2+}$ (**14**) (DMB = 4,4′-dimethyl-2,2′-bipyridine) (Figure 8b), we can identify the main product from the photoirradiation as $Ru(bpy)_2DMB^{2+}$ (**14**). The isolation of the Ni^{II} complex after photocleavage was unsuccessful. We have thus postulated a mechanism to account for the photochemical processes (Scheme 3). The first step involves the reductive quenching of the excited state of **5** by ascorbate. Then, a

(23) Cl^-, Br^-, or I^- ion coordinates to the axial positions of Ni^{II}–cyclam to form 6-coordinate Ni^{II} center in the presence of these ions, and so the distribution of the high-spin state increases (see ref 13).

Scheme 3

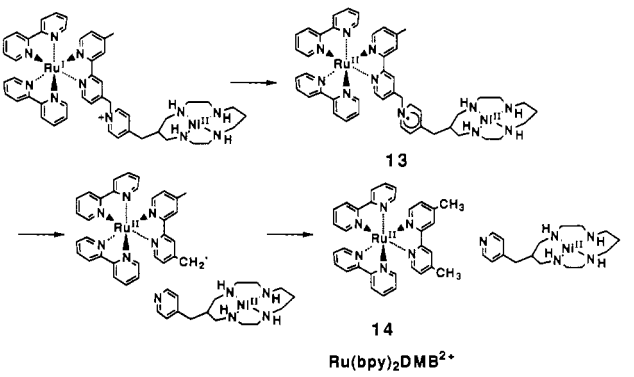

pyridinium radical, **13**, is produced to cause homolytic cleavage at the benzylic position. The generated radical is then reductively quenched by ascorbate and subsequently $Ru(bpy)_2DMB^{2+}$ (**14**) is formed.

Although the reductive photocleavage of **5** occurred in the presence of a reductant, we determined the catalytic efficiency of CO_2 photoreduction by **5** under the same conditions (Table 2, run 19). Surprisingly, the evolved amount of CO is twice the amount obtained from run 1, and additionally, H_2 production is depressed. A more detailed mechanism for this effective photoreduction of CO_2 is now underway.

Conclusion

The synthesis of a Ru^{II}–Ni^{II} heteronuclear complex (**5**) and several Ni^{II}–cyclam complexes containing a pyridinium pendant (**4a–d**) has been accomplished. The coordination environment at the Ni^{II} centers of **4a–d** is essentially the same as in the parent Ni^{II}–cyclam (**1**). Electrochemical studies have revealed that complexes **4a–c** show both a one-electron reduction for a pyridinium cation to a pyridinium radical and a one-electron reduction for Ni^{II} to Ni^{I}. The reduction potential of the pyridinium cation is more positive than that of Ni^{II} to Ni^{I} and increases in the order **4a** < **4b** < **4c** due to the electron-withdrawing effect of the substituent on the N atom of the pyridinium moiety. This electron-withdrawing effect might be the key factor that governs the generation of the active species for the photoreduction of CO_2.

Complex **5** is an improved version of the Ru^{II}–Ni^{II} heteronuclear complexes in the light of several problems which were recognized from our previous work with **2** and **3**.[9] (1) The $Ru(bpy)_3^{2+}$ subunit in **5** is attached to Ni^{II}–cyclam at the 4-position of one bipyridine ligand via a pyridinium cation. For **2**, steric hindrance by the 6-methylene bridge caused an increase in the Ru–N bond distance and a decrease in the ligand field strength for the Ru^{II} moiety. These were the main causes of the short lifetime of the excited state of **2**. (2) The Ni^{II}–cyclam subunit in **5** is linked to $Ru(bpy)_3^{2+}$ at the C-6 position of the cyclam ring via the pyridinium cation. With the previous Ru^{II}–Ni^{II} complexes, **2** and **3**, each Ru^{II} complex was attached via an N atom on the cyclam. Alkylation of the N atom of cyclam changes the redox properties and the CO_2 reduction efficiency of the Ni^{II} complex. (3) The distance between the Ru^{II} center and the Ni^{II} complex is large enough to prevent the excited state of the $Ru(bpy)_3^{2+}$ subunit in **5** from being quenched by intramolecular energy transfer from the $Ru(bpy)_3^{2+}$ to the Ni^{II}–cyclam moiety. Energy transfer from the excited state of the $Ru(phen)_3^{2+}$ moiety to the high-spin Ni^{II}–cyclam of **3** might be the main reason for the short lifetime of its excited state.

The problems described above have been partially resolved with the current heteronuclear system. Although the reductive photocleavage of **5** occurs in the presence of ascorbate, possibly at the positively charged N atom of the pyridinium cation, the amount of CO evolved by **5** was twice that obtained from the separate system. Therefore, the design of a more stable link between the Ru^{II} and Ni^{II} moieties would dramatically improve this type of system.

Acknowledgment. This work was supported by Nissan Science Foundation and a Grant-in-Aid for Science Research (A) (No. 04403024) from the Ministry of Education, Science, and Culture in Japan, both for E.K. We are also grateful to the Medical Molecules Exploring Center at Hiroshima University School of Medicine.